Journal of King Saud University – Science 32 (2020) 2854–2862

Contents lists available at ScienceDirect

Journal of King Saud University – Science

journal homepage: www.sciencedirect.com

Original article

Deciphering the interaction of plumbagin with human serum albumin: A combined biophysical and molecular docking study

Faizan Abul Qais [a], Fohad Mabood Husain [b,*], Rais Ahmad Khan [c,*], Iqbal Ahmad [a], Iftekhar Hassan [d]

[a] Department of Agricultural Microbiology, Faculty of Agricultural Sciences, Aligarh Muslim University, Aligarh, India
[b] Department of Food Science and Nutrition, College of Food and Agriculture Science, King Saud University, Riyadh 11451, Saudi Arabia
[c] Department of Chemistry, College of Science, King Saud University, P.O. Box 2455, Riyadh 11451, Saudi Arabia
[d] Department of Zoology, College of Science, King Saud University, P.O. Box 2455, Riyadh 11451, Saudi Arabia

ARTICLE INFO

Article history:
Received 5 May 2020
Revised 26 June 2020
Accepted 12 July 2020
Available online 17 July 2020

Keywords:
Plumbagin
Human serum albumin
Interaction
Molecular docking

ABSTRACT

It is important to understand the nature and mechanism of interaction of drugs with serum albumins as such interactions govern their pharmacokinetics and pharmacodynamics. Plumbagin is a natural phytocompound, mainly present in the bark of Plumbaginaceae family plants and it has numerous therapeutic potentials. In this study, the interaction of plumbagin with human serum albumin (HSA) was deciphered using an array of biophysical and computational tools. The UV–vis spectroscopy established the formation of plumbagin-HSA complex with binding constant as 2.32×10^4 M^{-1}. Fluorescence spectroscopy revealed that there was static mode of quenching of HSA's fluorescence by plumbagin. The binding constant obtained by fluorescence spectroscopy was of the similar order as in case of UV–vis spectroscopy. The negative value of $\Delta H°$ (−3.67) indicated an endothermic nature of the reaction and negative value of $\Delta G°$ (−6.40 to −6.58) confirmed that complexation of plumbagin to HSA was spontaneous. There was nearly one binding site in HSA for plumbagin. Titration of plumbagin to HSA in presence of site-specific markers showed that plumbagin interacted at sub-domain IIA of HSA, commonly known as Sudlow's site I. Moreover, the binding resulted in changes in microenvironment of tryptophan while of tyrosine residues remained approximately unchanged. This interaction also resulted in decrease of α-helical content of the studied serum protein. FRET calculations revealed that distance between plumbagin and HSA's fluorophore (Trp214) was 2.27 nm. Finally, molecular docking studies substantiated the *in vitro* finding. Plumbagin formed hydrogen bond with Lys199 and Arg257 of HSA. Additionally, Arg222, His242, and Ala261 interacted *via* van der Waals forces and Leu238, Leu260, Ile264, Ile290, and Ala291 of HSA interacted with plumbagin through hydrophobic forces.

1. Introduction

Human serum albumin (HSA) is a model protein to study the interactions of biological macromolecules with drugs and it does not exhibit toxicity and immunogenicity (Shahabadi and Maghsudi, 2009). HSA performs an array of functions including distribution, deposition of endogenous and exogenous molecules; maintenance of blood's osmotic pressure; and transportation of drugs to the molecular target (Yasmeen et al., 2017). There are three homologous domains (I, II and III) of HSA which is further subdivided two sub-domains, i.e. A and B. The most commonly characterized sites of HSA known for ligand binding are located in sub-domain IIA and IIIA also referred as Sudlow's site I and Sudlow's site II, respectively (Sudlow et al., 1975). Most of the drugs usually interact with HSA *via* non-covalent interactions. These drugs interact reversibly with the hydroxyl, carboxyl or different binding groups located on the amino acids residues of HSA *via* hydrogen bond, van der Waal's forces, hydrophobic interactions, and ionic interactions (Zia et al., 2018). Drugs showing weak

Abbreviations: CD, Circular dichroism; HSA, Human serum albumin; FRET, Förster resonance energy transfer.

* Corresponding authors.
E-mail addresses: fhusain@ksu.edu.sa (F.M. Husain), krais@ksu.edu.sa (R.A. Khan).

Peer review under responsibility of King Saud University.

Production and hosting by Elsevier

https://doi.org/10.1016/j.jksus.2020.07.008
1018-3647/

binding affinity to the carrier protein have short life-span in serum and their distribution is poor; while drugs exhibiting greater binding affinity are relatively more efficacious (Hall et al., 2013). Hence, the nature and strength of interaction of drugs with serum albumins is a vital parameter to be considered to study as it determines its pharmacodynamics and pharmacokinetics (Sułkowska, 2002). The information regarding the binding strength, number of binding sites, structural alterations induced in protein due to interaction yield useful details about the clearence and pharmacological distribution of the drugs.

Plumbagin (5-hydroxy-2-methyl-1,4-naphthoquinone), belonging to naphthoquinone family of compounds, is an important member of quinone family which is found in leaf, stem bark, and root of many plant families such as Dioncophyllaceae, Plumbaginaceae, Ebenaceae, and Ancistrocladaceae. The phytocompound is reported to exhibit anticancer, antioxidant, anti-inflammatory, antibacterial, hypolipidemic, antifungal, and neuroprotective activities (Liu et al., 2017). The therapeutic application of plumbagin is limited mainly due to the low solubility in aqueous solutions. The nanoformulation based on drug carrier systems may be a novel approach to enhance the bioavailability and thereby increasing the clinical application (Bothiraja et al., 2013). Researchers have developed many drug carrier systems for the effective delivery of plumbagin for improved anticancer efficacy (Duraipandy et al., 2014).

The present study focuses on the elucidation of binding mode of plumbagin with HSA that was achieved using numerous biophysical and computational tools. The UV–vis spectroscopy confirmed the plumbagin-HSA complex formation. Fluorescence quenching study was performed to obtain the quenching mode and values of various thermodynamic parameters. Site-specific marker experiment was done to get the exact binding site of plumbagin in HSA. Circular dichroism analysis was carried out to study the alterations in the secondary structural content of the studied serum protein. Finally, molecular docking studies substantiated the *in vitro* finding and provided detailed information regarding the interacting amino acids.

2. Materials and methods

2.1. Materials

Human serum albumin (HSA) free from fatty acids (A3782), warfarin (258016), ibuprofen (I110), and plumbagin (P7262) were procured from Sigma-Aldrich, USA. All other reagents and chemicals used in this present study were checked for analytical grade before using.

2.2. Preparation of stock solutions

The solution of HSA (300 μM) was prepared in phosphate buffer (10 mM, pH 7.4). The stock solution (1 mM) of plumbagin was prepared in DMSO. The solution of warfarin and ibuprofen (6 mM each) was made in HPLC grade ethanol. The dilution of the stock solutions was made in phosphate buffer otherwise stated.

2.3. UV–visible spectroscopy

The UV–vis spectroscopy was carried out using UV-2600 spectrophotometer, Shimadzu, Japan. Briefly, an increasing concentration of plumbagin (3–24 μM) was consecutively added to a fixed concentration (7.5 μM) of the human serum albumin (HSA). All spectral recordings were taken at 298 K and dilutions were made in phosphate buffer. The baseline correction was performed using phosphate buffer. All the absorption spectra were recorded in 200–400 nm range.

2.4. Steady state fluorescence

The fluorescence emission spectra of the samples were recorded using Shimadzu 5301-PC spectrofluorometer, Japan, in quartz cuvette of 1.0 cm path length. The excitation of HSA and plumbagin-HSA complex was done at 280 nm and emission spectra were obtained in 290–600 nm. HSA (3 μM) concentration was fixed and a varying concentration (0.5–4.0 μM) of plumbagin was titrated. The experiment was performed at three different temperatures to quantify the values of various thermodynamic parameters.

2.5. Competitive displacement assay

To obtain the precise site of binding of a molecule in a protein, certain markers of known site-specific binding are used. In competitive displacement assay, 6 μM cite marker was added to 3 μM HSA to saturate all the binding sites present in HSA. The site marker-HSA mixture was excited at 280 nm and emission spectra were recorded in the absence and presence of plumbagin (0.5–4.0 μM) in 290–550 nm range. This experiment was done separately for ibuprofen and warfarin as mentioned previously (Ishtikhar et al., 2014b).

2.6. Assessment of ionic interactions

This assay was performed to elucidate whether the ionic interactions are involved in the formation of HSA-plumbagin complex. Fluorescence emission signal of HSA (3 μM) was recorded in the absence and presence (0.5–4.0 μM) of plumbagin by exciting at 280 nm in phosphate buffer. The emission spectra was recorded form 290 to 550 m. The experiment was repeated at varying concentrations (0, 50, and 100 mM) of NaCl.

2.7. Synchronous fluorescence studies

Synchronous fluorescence assay was performed to find out the alterations in the microenvironment of aromatic amino acids (mainly tryptophan and tyrosine). In this experiment, the difference between emission and excitation wavelengths ($\Delta\lambda$) are kept fixed. A varying concentration of plumbagin (5–40 μM) was added to the fixed amount of HSA (3 μM). The $\Delta\lambda$ = 15 nm was set for tyrosine residue in which excitation and emission wavelengths were set from 240 and 255 nm, respectively. Likewise, $\Delta\lambda$ = 60 nm was fixed tryptophan residue where the excitation and emission wavelengths were 240 nm and 300 nm.

2.8. Circular dichroism (CD) measurements

The CD spectra of HSA and HSA-plumbagin complex were recorded using J-815 JASCO spectropolarimeter. The spectra of free HSA (7 μM), HSA-plumbagin complex (1:1 and 1:2 molar ratios) were recorded at 25 °C using thermostatically controlled cell holder. The spectra in this study are the average of three scans. One mm quartz cuvette was used in far-UV CD analysis.

2.9. Förster resonance energy transfer (FRET)

For FRET, fluorescence emission signal of HSA (10 μM) and absorption spectrum of plumbagin (10 μM) were recorded. The spectral overlap was calculated using PhotochemCAD™ software. The normalized overlap of absorption and emission spectrum were used to for the calculation of critical distance and energy transfer

efficiency (E) as per the Förster's theory (Forster and Sinanoglu, 1965).

2.10. Three-dimensional fluorescence spectroscopy

All 3D fluorescence spectra were recorded using Shimadzu spectrofluorophotometer RF-6000, Japan. The 3D fluorescence emission signals of HSA (5 μM) and HSA-plumbagin complex (1:2 molar ratio) were recorded at room temperature. The emission and excitation wavelengths were 200–500 nm and 200–400 nm, respectively.

2.11. Molecular docking

The *in silico* interaction between HSA and plumbagin was performed by using AutoDock Vina (Trott and Olson, 2009). AutoDock-vina performs faster and is also known to do more accurate calculations than AutoDock 4. The structure of HSA was obtained from Protein Data Bank (www.rcsb.org) [PDB ID: 1AO6]. The water molecules in the coordinate file of HSA were deleted using MGL Tools-1.5.4 (Morris et al., 1998). The merging of non-polar hydrogen atoms was performed along with the addition of Kollman charges to the receptor molecule. The grid centre was fixed to x = 22.717, y = 33.725, and z = 38.864 with grid size as 52 × 48 × 48 Å. The receptor molecule was then saved in pdbqt format. The three-dimensional conformer of plumbagin [CID: 10205] was obtained from PubChem website in SDF format and converted to PDB format using Chimera 1.14. The roots of ligand molecule were detected using MGL Tools to make it flexible and the coordinate was then saved in pdbqt format. The other parameters of docking were left as default and post docking assessment was done using Discovery Studio, PyMol 2.2.3, and LigPlot^{+}. The solvent accessible surface areas (ASA) of HSA and plumbagin-HSA complex were obtained from online server (http://cib.cf.ocha.ac.jp/bitool/ASA) available from Center for Informational Biology, Ochanomizu University.

3. Results and discussion

3.1. UV–vis spectroscopy

UV–vis absorption spectroscopy is an important tool to evaluate the changes induced in protein by the interaction of ligand. The absorption spectra of the protein in the absence and presence of plumbagin is shown in Fig. 1A. The characteristic absorption profile of HSA exhibits two absorption maxima, one at 218 nm and other at 280 nm. The absorption maxima near to 220 nm is due to the framework conformation of HSA while the peak near 280 nm is due to the $\pi \rightarrow \pi^*$ transition of aromatic amino acids *viz.* Tyr, Phe, and Trp (Mohammadi et al., 2017). The successive addition of plumbagin resulted in decrease in absorption at 218 nm along with the red shift of approximately 14 nm. This change indicates the formation of complex between HSA and plumbagin that leads to the conformational alterations in the framework of HSA. On contrary, the peak at 280 nm slightly increased indicating a slight change on the conformation of aromatic amino acids due to the interaction of plumbagin (Lou et al., 2017).

The quantitative analysis of UV–vis spectroscopic data was performed using equation-1 (Qais et al., 2016):

$$\frac{1}{A-A_0} = \frac{\varepsilon_{HSA}}{\varepsilon_B} + \frac{\varepsilon_{HSA}}{\varepsilon_B K} \times \frac{1}{C} \quad (1)$$

where A_0 and A are λ_{max} of HSA without and with plumbagin; C is the concentration of plumbagin; ε_{HSA} and ε_B are molar extinction coefficient of HSA and plumbagin-HSA complex; and K is binding constant. The binding constant was calculated form double reciprocal plot as shown in Fig. 1B. The binding constant was found to be 2.32×10^4 M^{-1}. The calculation of Gibb's free energy was done using the following equation-2 (Khatun et al., 2019):

$$\Delta G^0 = -RT \ln K \quad (2)$$

where, ΔG° is Gibb's free energy; T in temperature; R is universal gas constant; and K is binding constant. The ΔG° value was obtained as −5.95 kcal mol^{-1}. The negative sign of ΔG° confirms the spontaneous nature of the interaction between plumbagin and HSA.

3.2. Steady state fluorescence

The fluorescence spectroscopy was deployed to assess the binding of plumbagin with HSA. The fluorescence emission spectra of HSA and HSA-plumbagin complexes is shown in Fig. 2A. It is clear from the data that HSA exhibited emission maximum at 335 nm when excited at 280 nm. The titration of plumbagin to HSA resulted in a progressive fluorescence quenching of the protein with a blue shift to 321 nm. This florescence quenching and blue shift caused by plumbagin indicates the formation of HSA-plumbagin complex. The quantitative analysis of fluorescence emission data was done using Stern–Volmer equation-3 (AlAjmi et al., 2020):

$$\frac{F_0}{F} = 1 + K_{SV}[Q] \quad (3)$$

where F_0 is free HSA's fluorescence; F is fluorescence of HSA-plumbagin complex; K_{SV} is Stern–Volmer constant; and [Q] is concentration of plumbagin. The Stern–Volmer plot is presented in

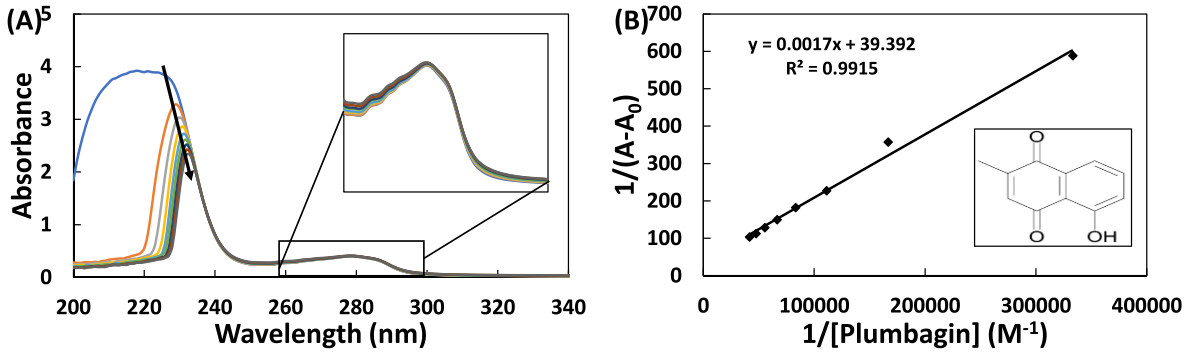

Fig 1. (A) UV–vis absorption spectra of HSA in the absence and presence of different concentrations of plumbagin, enlarged portion of 260–300 nm (inset); (B) double inverse plot, structure of plumbagin (inset). The concentration of HSA and plumbagin was 7.5 μM and 3–24 μM respectively.

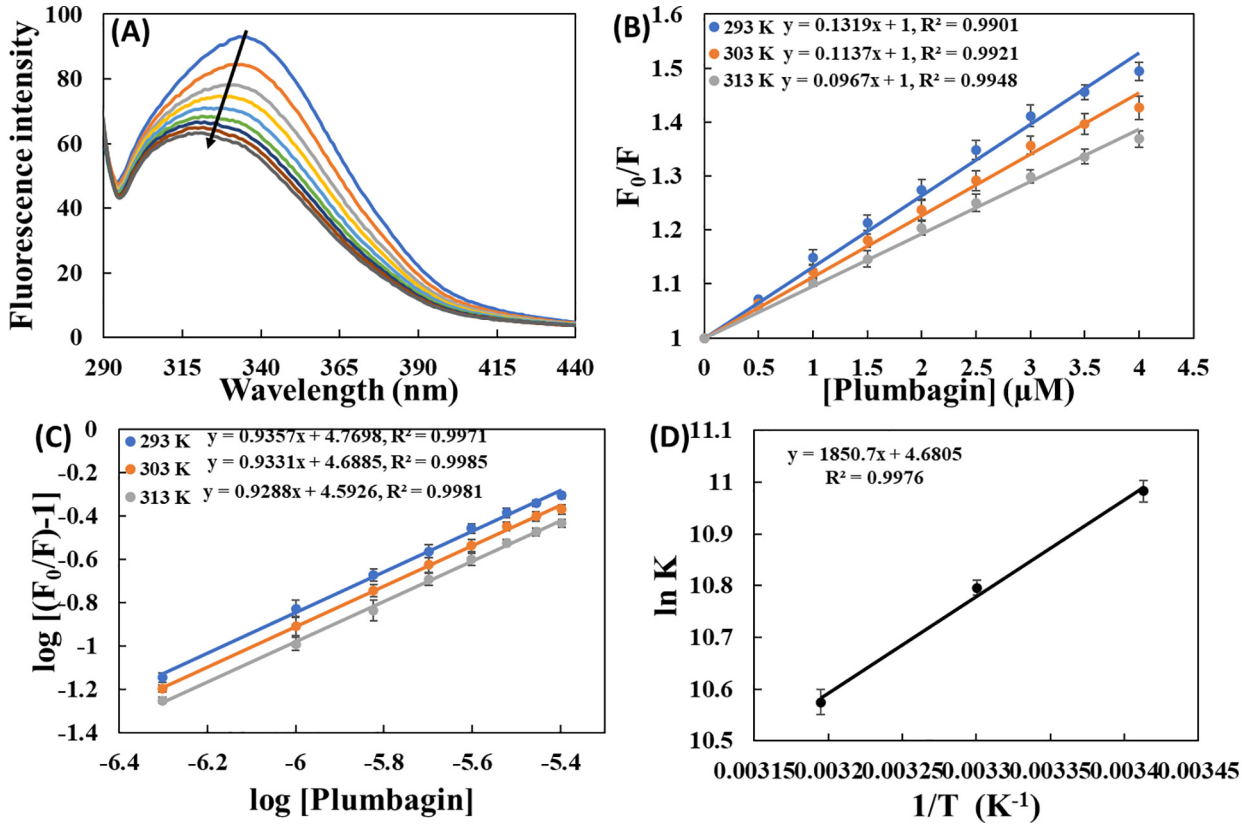

Fig 2. (A) Fluorescence emission signals of HSA and HSA-plumbagin complex at varying concentrations; (B) Stern–Volmer plots for the interaction of plumbagin with HSA at varying temperatures; (C) Double log plot for interaction of plumbagin with HSA; (D) Van't Hoff plot. The concentration of HSA and plumbagin was 3 μM and 0.5–4.0 μM respectively.

Fig. 2B. The slope of this plot yielded the value of Stern–Volmer constant which is enlisted in Table 1. The K_{SV} was found to be in the range of 09.67–13.12 × 10^4 M^{-1}. The quenching mode (static or dynamic) cannot be ascertained the value of K_{SV}. Hence, quenching rate constant (K_q) was calculated using equation-4 (Iqbal et al., 2018):

$$K_q = \frac{K_{SV}}{\tau_0} \quad (4)$$

where, τ_0 the fluorescence lifetime of tryptophan (~5.78 × 10^{-9} s) (Ishtikhar et al., 2014a); and K_q is quenching rate constant. The K_q value ranged from 1.67 × 10^{13} to 2.28 × 10^{13} M^{-1} s^{-1} which is presented in Table 1. In static quenching mode, there is direct interaction between the excited a molecule through chemical bonds. On contrary, the quencher indirectly interacts with the molecule in dynamic quenching (Gao et al., 2004). The value of K_q in case of maximum scatter collision quenching constant of a biomolecule is greater than 2.0 × 10^{10} M^{-1} s^{-1} (Qais et al., 2016). K_q values deciphers the quenching mode to be static. The quenching mode can also be validated by dependence of K_{SV} values with temperature. For dynamic quenching, the K_{SV} value increases with temperature, on contrary the trend is reverse in case of static quenching. For plumbagin-HSA interaction, there was decrease in K_{SV} values with increasing temperature, further validating the static mode of quenching.

3.3. Determination of thermodynamic and binding parameters for plumbagin and HSA interaction

The values of the number of binding sites (n) and binding constants (K) were obtained using the equation-5 (Nusrat et al., 2018):

$$\log\frac{F_0 - F}{F} = \log K + n\log[Q] \quad (5)$$

where, K is binding constant; and n is number of binding sites. The slope of double log plot yielded the values of n and y-axis intercept gave the values of binding constants (Fig. 2C). The values of K were found to be 5.93 × 10^4, 4.90 × 10^4, and 3.96 × 10^4 M^{-1} at 298, 303, and 313 K, respectively. The n remained nearly one indicating that plumbagin preferentially has one binding site in HSA. Binding constant and n obtained at three temperatures is mentioned in Table 1. The data makes it obvious that the binding constant decreased with increasing temperature indicating that HSA-plumbagin complex was relatively more stable at lower temperature compared to physiological temperature.

Table 1
The values of Stern–Volmer constant, quenching rate constant, binding constant and number of binding for the binding of plumbagin with HSA at different temperatures.

Temp (K)	K_{sv} (×10^4 M^{-1})	K_q (×10^{13} M^{-1} s^{-1})	R^2	K (×10^4 M^{-1})	n
293	13.12 ± 0.57	2.28 ± 0.09	0.9901	5.93 ± 0.94	0.935 ± 0.016
303	11.51 ± 0.39	1.99 ± 0.06	0.9921	4.90 ± 0.54	0.933 ± 0.009
313	09.67 ± 0.45	1.67 ± 0.07	0.9948	3.96 ± 0.77	0.928 ± 0.014

The values of binding constant at different temperatures were used for the assessment of thermodynamics of the HSA-plumbagin complex formation. In case of drug-protein interactions, non-covalent forces such as van der Waals forces, hydrophobic interactions, hydrogen bonds and electrostatic interactions are predominant (Khan et al., 2008). The values of thermodynamic parameters and their mathematical sign suggest the nature forces responsible for the binding. The values of enthalpy and entropy change were obtained from van't Hoff's plot using equation-6:

$$\ln K = -\frac{\Delta H^{\circ}}{RT} + \frac{\Delta S^{\circ}}{R} \quad (6)$$

where, K is binding constant, ΔS° is entropy change, R is universal gas constant, and ΔH° is enthalpy change, and T is temperature. The van't Hoff's plot is shown in Fig. 2D and values of ΔS° and ΔH° is given in Table 2. The negative value of ΔH° is indication of endothermic nature of the interaction process. Moreover, positive value of ΔS° suggests the randomization of water molecules after interaction (Khan et al., 2008). A positive ΔS° value is also indicative of the involvement of hydrophobic interactions (Wang et al., 2007).

The value of Gibb's free energy change (ΔG°) was obtained using equation-7 (Abdel-Rahman et al., 2019):

$$\Delta G^{\circ} = \Delta H^{\circ} - T\Delta S^{\circ} \quad (7)$$

The ΔG° was obtained in −6.40 to −6.58 kcal mol^{-1} range. Its negative value shows that the binding of plumbagin to HSA was spontaneous reaction (Li et al., 2007).

3.4. Evaluation of binding site of plumbagin in HSA

It has been deciphered from HSA's crystal structure that there are 3 homologous domains named I, II, and III. Each one of these domains is divided into two sub-domains i.e. A and B. To obtain site of binding of drug molecules in HSA, some site-markers with known binding site are used. Crystallographic studies have confirmed that warfarin binds at Sudlow's site I (sub-domain IIA) and ibuprofen binds at Sudlow's site II (sub-domain IIIA) of HSA (Sudlow et al., 1975). Stern–Volmer plot was made for comparative assessment of binding of plumbagin in the absence and presence of site markers using equation-3 as shown in Fig. 3A. The K_{SV} values obtained in site-specific marker experiment is enlisted in Table 3. The data showed that K_{SV} value slightly changed in presence of ibuprofen indicating that plumbagin did not compete for Sudlow's site II and hence have different binding site. On contrary, K_{SV} value remarkably decreased when warfarin was present with HSA. The finding illustrates that plumbagin has competence for binding site as that of warfarin. Moreover, a comparison of the titration results was plotted in terms of relative fluorescence intensity (Fig. 3B). A small change in fluorescence quenching behaviour was observed in presence of ibuprofen. However, there was relatively larger change in fluorescence quenching behaviour of HSA in presence of warfarin suggesting that binding site of plumbagin was same as that of warfarin. Site-marker experiment confirmed that plumbagin interacted at sub-domain IIA of HSA.

3.5. Synchronous fluorescence spectroscopy

The steady state fluorescence data only gives information about the binding constant and various thermodynamic parameters. Synchronous fluorescence analysis data gives information regarding the changes in molecular environment of fluorophores of HSA caused by the binding of drugs (Ibrahim et al., 2010). Any shift (blue shift or red shift) in the fluorescence emission maximum gives valuable information about the alterations of polarity around the fluorophore of HSA (Akram et al., 2020). There is concurrent excitation and emission in synchronous fluorescence, in which their difference ($\Delta\lambda$) is kept constant. $\Delta\lambda$ at 60 nm gives information regarding the changes in the microenvironment of tryptophan, whereas $\Delta\lambda$ = 15 nm gives information about the microenvironment of tyrosine (Miller, 1979).

The synchronous fluorescence signals of HSA and HSA-plumbagin complex is shown in Fig. 3C and D. There was a negligible shift in the fluorescence emission maxima of HSA at $\Delta\lambda$ = 15 (Fig. 3C). This indicates that microenvironment around tyrosine was not changed remarkably. However, at $\Delta\lambda$ = 60 nm (Fig. 3D), there was 2 nm red shift showing that polarity in the vicinity of tryptophan residue was increased and thereby decreasing the hydrophobicity around this amino acid (Kragh-Hansen, 1981). The emission at 330 nm indicates that tryptophan residue is present near or in close vicinity of non-polar region of HSA (Miller, 1979). The binding of plumbagin has caused the exposure of tryptophan residue to the surrounding water molecules (Bolattin et al., 2016). The synchronous studies deciphered that microenvironment of tryptophan was changed after interaction of plumbagin while of tyrosine remained approximately same.

3.6. Effect of NaCl

This assay gives information about the involvement of ionic interactions in plumbagin-HSA complex formation. The double log plot for HSA's fluorescence quenching by plumbagin in the presence and absence of NaCl is presented in Fig. 4A. In absence of NaCl, binding constant was obtained as 3.55×10^4 M^{-1}. In presence of 50 and 100 mM NaCl, the binding constant was obtained as 3.51 and 3.49×10^4 M^{-1} respectively. A negligible alteration in the value of binding constant signifies that there was insignificant involvement of ionic interactions in the binding of plumbagin with HSA.

3.7. Circular dichroism spectroscopy

CD is a very sensitive and routinely used tool to study the secondary structure of a protein. The CD spectra of HSA in the absence and presence of plumbagin is shown in Fig. 4B. In a typical CD spectrum of HSA, two negative peaks at 208 and 222 nm are due to the α-helical content of the protein (Zaman et al., 2019; Zhang et al., 2008). CD results are presented in mean residue ellipticity (MRE) which was calculated using equation-8 (Alam et al., 2017):

$$\text{MRE} = \frac{\text{observed CD(mdeg)}}{C_p nl \times 10} \quad (8)$$

Table 2
The thermodynamic parameters for the interaction of plumbagin with HSA at various temperatures.

pH	Temp (K)	ΔG (kcal mol^{-1})	ΔH (kcal mol^{-1})	TΔS (kcal mol^{-1})	R^2
7.4	293	−6.40 ± 0.38		2.72 ± 0.13	0.9876
	303	−6.49 ± 0.32	−3.67 ± 0.21	2.81 ± 0.14	
	313	−6.58 ± 0.39		2.91 ± 0.14	

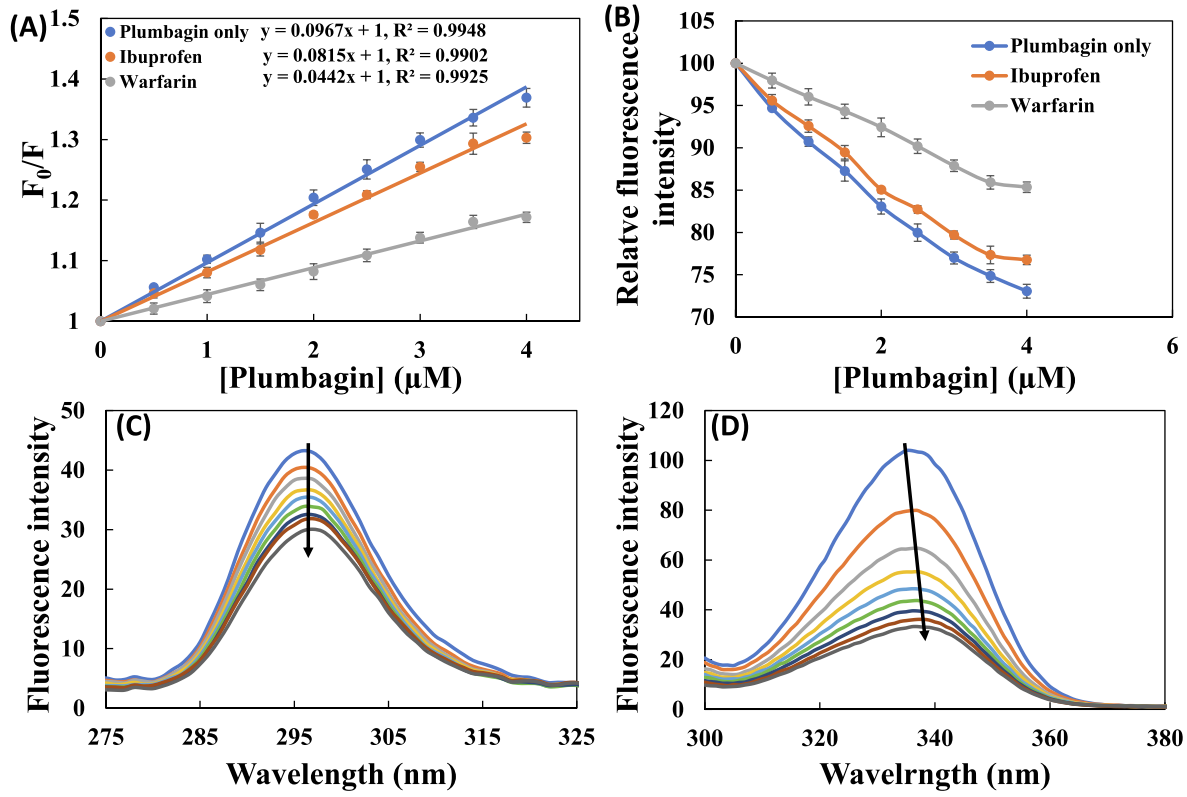

Fig 3. (A) Stern–Volmer plot for plumbagin-HSA interaction in the absence and presence of different site markers; (B) Plots showing plumbagin induced quenching of HSA's fluorescence in presence of site markers; (C) Synchronous fluorescence spectra of human serum albumin HSA (3 μM) in the absence and presence of plumbagin (5–40 μM) at Δλ = 15 nm; (D) Synchronous fluorescence spectra of human serum albumin HSA (3 μM) in the absence and presence of plumbagin (5–40 μM) at Δλ = 60.

Table 3
The Stern-Volmer constant (K_{sv}) of fluorescence quenching of HSA by plumbagin in absence and presence of site markers.

Site Marker	K_{sv} ($\times 10^4$ M^{-1})	R^2
No site marker	9.67 ± 0.45	0.9948
Ibuprofen	8.14 ± 0.29	0.9902
Warfarin	4.41 ± 0.32	0.9925

where, n is number of amino acids; C_p is concentration of the protein; and l is path length of cuvette. The percent of α-helix in free HSA and plumbagin-HSA complex was calculated using equation-9 (Alam et al., 2017):

$$\%\alpha - \text{helix} = \frac{(-\text{MRE}_{208} - 4000)}{33000 - 4000} \times 100 \quad (9)$$

where, MRE_{208} is MRE at 208 nm. The MRE_{208} and percent α-helix in HSA at varying concentrations of plumbagin is mentioned in Supplementary Table S1. As evident from the results, there was 57.99% α-helix in free HSA which corroborates with previous finding (Ali et al., 2017). The presence of plumbagin caused a decrease in intensity at the negative peaks of HSA. A decreased elliptical intensity indicates the reduction of α-helix of HSA caused by the interaction of plumbagin. At 1:1 and 1:2 M ratios, % α-helix was obtained as 50.37 and 47.29% respectively. Moreover, the peak shape and position of plumbagin-HSA complexes remained approximately same, indicating that basic conformation of HSA was nearly same even after interaction (Bhogale et al., 2013).

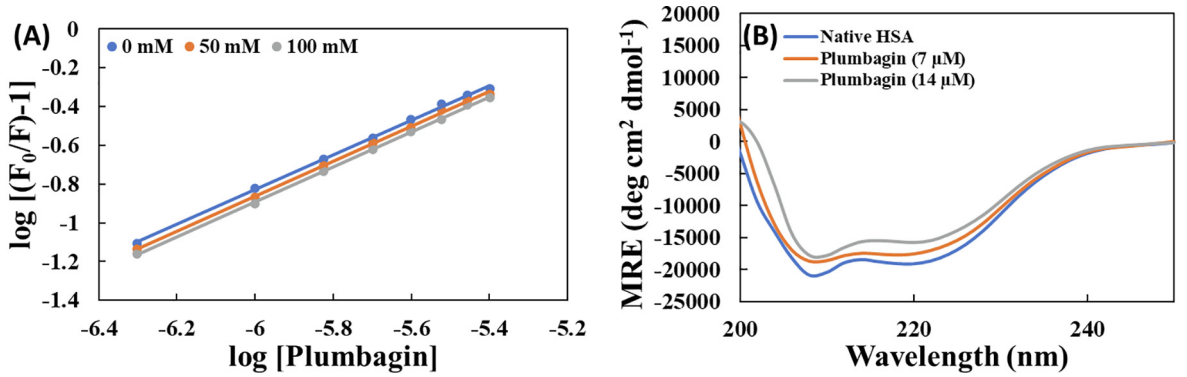

Fig 4. (A) Double plot for the binding of plumbagin with HSA in the absence and presence (50 and 100 mM) of NaCl; (B) Far UV-CD spectra HSA and plumbagin-HSA complex at varying concentrations (1:0, 1:1 and 1:2).

3.8. 3-D fluorescence analysis

Three-dimensional fluorescence spectroscopy provides information about the structural and conformational changes occurred in a protein due to binding of small molecules such as drugs (Siddiqui et al., 2019). The bird's eye view and corresponding contour diagram of HSA in the absence and presence of plumbagin is shown in Supplementary Fig S1. Peak 'A' of 3-D fluorescence spectrum of HSA is because of Rayleigh scattering while peak 'B' is related to the characteristic of aromatic amino acids (Kabir et al., 2016). The presence of plumbagin decreased the fluorescence intensity of HSA at peak 'A' indicating the formation of HSA-plumbagin complex. The fluorescence emission maxima data is presented in Table 4. Moreover, the reduction in fluorescence intensity also depicts that the overall diameter of HSA decreased by the interaction of plumbagin, which in turn caused the reduction of the scattering effect (Siddiqui et al., 2019). The fluorescence signal at peak 'B' of the protein also decreased remarkably in presence of plumbagin suggesting the conformational changes around tyrosine and tryptophan residues (Suryawanshi et al., 2016). The results support the findings that the binding of plumbagin with HSA induced changes in the microenvironment of aromatic amino acids and conformational alterations in the protein.

3.9. Förster resonance energy transfer (FRET)

Using FRET, distance between two interacting molecules and energy transfer efficiency could be calculated. For a successful FRET, the fluorescence emission band of donor molecule (HSA) should overlap with the absorption of acceptor (plumbagin). FRET only takes place when; i) the acceptor and donor molecules are in close propinquity, ii) the donor should possess high quantum yield, and iii) there must be proper orientation of transition dipole moment (Xu et al., 2011). If absorption spectrum of plumbagin overlaps substantially with HSA's emission spectrum, there is higher chances of energy transfer (Forster and Sinanoglu, 1965). The spectral overlap of HSA and plumbagin is presented in Supplementary Fig S2. The degree of energy transfer efficiency is directly correlated the extent of spectral overlap. Energy transfer efficiency was calculated using equation-10 (Il'ichev et al., 2002):

$$E = 1 - \frac{F}{F_0} = \frac{R_0^6}{R_0^6 + r^6} \tag{10}$$

where, E is energy transfer efficiency; r is distance between acceptor and donor; and R_0 is the critical distance. The R_0 value was calculated using equation-11 (Khan et al., 2020):

$$R_0^6 = 8.79 \times 10^{-25} K^2 n^{-4} \phi J \tag{11}$$

where, K^2 is orientation factor (2/3); ϕ is the fluorescence quantum yield (0.118); J is degree of spectral overlap; and n is refractive index of medium (1.336) (Cyril et al., 1961). The degree of spectral overlap was calculated using equation-12:

$$J = \frac{\int_0^\infty F(\lambda)\varepsilon(\lambda)\lambda^4 d\lambda}{\int_0^\infty F(\lambda) d\lambda} \tag{12}$$

where $F(\lambda)$ is fluorescence of HSA in wavelength range from λ to $\lambda + \Delta\lambda$ and $\varepsilon(\lambda)$ is molar absorptivity of plumbagin at λ.

The values of spectral overlap and critical distance was obtained as 2.64×10^{-15} cm^3 L mol^{-1} and 1.96 nm respectively. The distance between Trp214 of HSA and plumbagin was obtained as 2.27 nm with efficiency of energy transfer as 29.04%. The values obtained in FRET using above-mentioned equations are enlisted in Supplementary Table S2. According to Förster's theory, the maximum R_0 value lies between 5 and 10 nm and the maximum r value ranges from 7 to 10 nm (Chen et al., 1990). The obtained values suggested a high probability of energy transfer from HSA to plumbagin. Moreover, these values also indicate that there was static quenching mode of energy transfer that caused an obvious reduction in fluorescence intensity of HSA (Chi et al., 2010).

3.10. Molecular docking

In silico binding analysis tools such as molecular docking and simulation play an important role in the development of new drugs as these tools elucidate the binding site of drugs to biological macromolecules (Rohs, 2005). The advantage of such techniques are that it takes lesser time and provide a thorough information about the interaction of ligand and receptor both in terms of binding energy and affinity compared to other techniques (Elokely and Doerksen, 2013). Most of times, *in silico* results corroborates with *in vitro* and *in vivo* findings. The structure of HSA was kept rigid while plumbagin was made flexible to attain the energetically most stable conformation. AutoDock Vina yielded nine different binding conformations with different binding energies. The docked conformation having lowest binding energy was used for analysis and discussed in this study. The docked conformation with minimum binding energy is presented in Fig. 5. The binding energy of best conformation was obtained as −7.7 kcal mol^{-1} which corroborates with the spectroscopic results. The binding site of plumbagin in HSA was present in sub-domain IIA of HSA which further corroborates the site-marker studies. Plumbagin formed two hydrogen bonds with Lys199 and Arg257 at distance of 2.50 and 4.40 Å, respectively. Moreover, Arg222, His242, and Ala261 interacted *via* van der Waals forces. Leu238, Leu260, Ile264, Ile290, and Ala291 of HSA interacted with plumbagin through hydrophobic forces. The details of the interaction are given in Table 5. The *in silico* results corroborated the experimental results and strengthened our findings.

The ASA of free HSA was found to be 54957.69 $Å^2$. The binding of plumbagin to HSA reduced the total ASA to 54775.7 $Å^2$ further validating the interaction of plumbagin to HSA. The maximum decrease in ASA of the interacting amino acids were Ala291, Leu238, Lys199, Ile290, Arg222, Leu260, and Arg257 by 33.42, 30.07, 18.30, 12.97, 11.93, 10.89, and 10.13 $Å^2$ respectively as shown in Supplementary Table S3.

4. Conclusion

The findings of this study provide useful information regarding the interaction of plumbagin with HSA. There was progressive quenching of fluorescence of HSA by plumbagin. The binding constant obtained by fluorescence spectroscopy ranged from 3.96 to 5.93×10^4 M^{-1}. The negative value of ΔH° suggested that the binding of plumbagin to HSA was endothermic reaction. Moreover, ΔG° value established that the binding process was spontaneous in nature and thermodynamically favourable. The molecular docking study deciphered that the forces responsible complexation were hydrogen bonds, hydrophobic interactions, and van der Waals forces. There was overall decrease in the solvent accessible surface area of HSA after the binding. These findings are significant to understand the nature interaction of plumbagin with HSA at molecular level and will assist in biomedical and pharmaceutical research.

Declaration of Competing Interest

The authors declare that they have no known competing financial interests or personal relationships that could have appeared to influence the work reported in this paper.

Table 4
Three-dimensional fluorescence signals for HSA and HSA-plumbagin complex.

Peak No.	Peak Position $\lambda_{ex}/\lambda_{em}$ (nm/nm)	Stokes Shift $\Delta\lambda$ (nm)	HSA only	HSA-plumbagin (1:2)	
			F_0	F	F_0/F
Peak A	280/330	50	24192.6	21763.0	1.11
Peak B	230/330	100	9493.1	4162.0	2.28

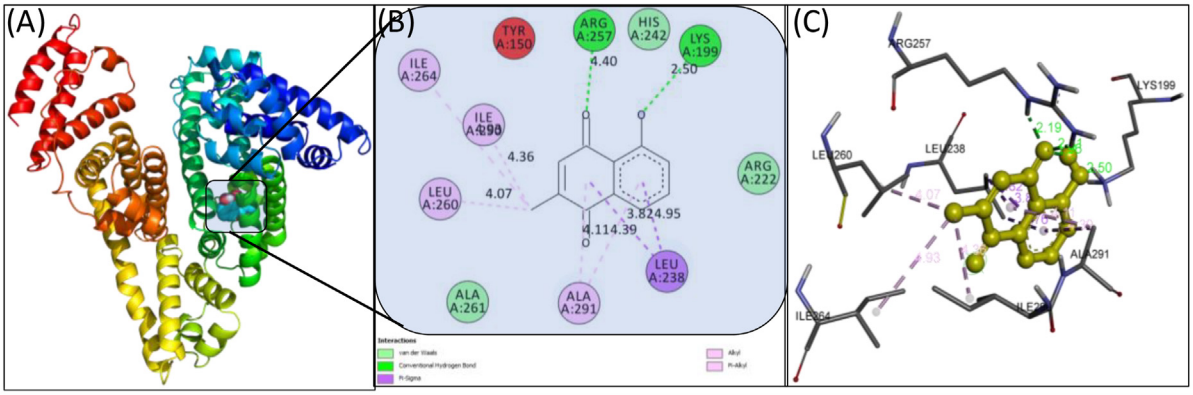

Fig 5. (A) Molecular docked model of plumbagin-HSA complex; (B) A 2D view obtained by Discovery Studio; (C) Plumbagin is shown with interacting amino acids of HSA.

Table 5
Predicted bonds between plumbagin and interacting amino acids of HSA.

S. No.	Amino acid	Distance (A°)	Nature of interaction	sub-domain
1.	Lys199	2.50	Hydrogen bond	IIA
2.	Arg257	4.40	Hydrogen bond	IIA
3.	Leu238		Hydrophobic interaction	IIA
4.	Leu260		Hydrophobic interaction	IIA
5.	Ile264		Hydrophobic interaction	IIA
6.	Ile290		Hydrophobic interaction	IIA
7.	Ala291		Hydrophobic interaction	IIA
8.	Arg222,		Van der Waal forces	IIA
9.	His242		Van der Waal forces	IIA
10.	Ala261		Van der Waal forces	IIA

Acknowledgements

The authors extend their appreciation to the Deanship of Scientific Research at the KSU for funding this work through research group project number RG-1440-059. FAQ is thankful to CSIR, New Delhi, India [File no. 09/112(0626)2k19 EMR] for providing senior research fellowship (SRF).

Conflict of interest

All the authors declare that there is no conflict of interest.

Appendix A. Supplementary data

Supplementary data to this article can be found online at https://doi.org/10.1016/j.jksus.2020.07.008.

References

Abdel-Rahman, L.H., Abu-Dief, A.M., Hassan Abdel-Mawgoud, A.A., 2019. Development, structural investigation, DNA binding, antimicrobial screening and anticancer activities of two novel quari-dentate VO(II) and Mn (II) mononuclear complexes. J. King Saud Univ. - Sci. 31, 52–60. https://doi.org/10.1016/j.jksus.2017.05.011.

Akram, M., Ansari, F., Qais, F.A., Kabir-ud-Din, 2020. Binding of cationic Cm-E2O-Cm gemini surfactants with human serum albumin and the role of β-cyclodextrin. J. Mol. Liq. 312, 113365. https://doi.org/10.1016/j.molliq.2020.113365.

AlAjmi, M.F., Rehman, M.T., Khan, R.A., Khan, M.A., Muteeb, G., Khan, M.S., Noman, O.M., Alsalme, A., Hussain, A., 2020. Understanding the interaction between α-1-acid glycoprotein (AGP) and potential Cu/Zn metallo-drugs of benzimidazole derived organic motifs: A multi-spectroscopic and molecular docking study. Spectrochim. Acta Part A Mol. Biomol. Spectrosc. 225, 117457. https://doi.org/10.1016/j.saa.2019.117457.

Alam, M.M., Qais, F.A., Ahmad, I., Alam, P., Hasan Khan, R., Naseem, I., 2017. Multi-spectroscopic and molecular modelling approach to investigate the interaction of riboflavin with human serum albumin. J. Biomol. Struct. Dyn. https://doi.org/10.1080/07391102.2017.1298470.

Ali, K., Qais, F.A., Dwivedi, S., Abdel-Salam, E.M., Ansari, S.M., Saquib, Q., Faisal, M., Al-Khedhairy, A.A., Al-Shaeri, M., Musarrat, J., 2017. Titanium dioxide nanoparticles preferentially bind in subdomains IB, IIA of HSA and minor groove of DNA. J. Biomol. Struct. Dyn. 36, 2530–2542. https://doi.org/10.1080/07391102.2017.1361339.

Bhogale, A., Patel, N., Sarpotdar, P., Mariam, J., Dongre, P.M., Miotello, A., Kothari, D. C., 2013. Systematic investigation on the interaction of bovine serum albumin with ZnO nanoparticles using fluorescence spectroscopy. Colloids Surf. B Biointerfaces 102, 257–264. https://doi.org/10.1016/j.colsurfb.2012.08.023.

Bolattin, M.B., Nandibewoor, S.T., Joshi, S.D., Dixit, S.R., Chimatadar, S.A., 2016. Interaction of hydralazine with human serum albumin and effect of β-cyclodextrin on binding: insights from spectroscopic and molecular docking techniques. Ind. Eng. Chem. Res. 55, 5454–5464. https://doi.org/10.1021/acs.iecr.6b00517.

Bothiraja, C., Pawar, A.P., Mali, A.J., Shaikh, K.S., 2013. Improved pharmaceutical properties of surface modified bioactive plumbagin crystals. Int. J. Surf. Sci. Eng. 7, 181. https://doi.org/10.1504/IJSURFSE.2013.053708.

Chen, G., Huang, X., Xu, J., Wang, Z., Zheng, Z., 1990. No Title, in: Method of Fluorescent Analysis. Science Press, Beijing, pp. 2–122.

Chi, Z., Liu, R., Teng, Y., Fang, X., Gao, C., 2010. Binding of oxytetracycline to bovine serum albumin: spectroscopic and molecular modeling investigations. J. Agric. Food Chem. 58, 10262–10269. https://doi.org/10.1021/jf101417w.

Cyril, L., Earl, J., Sperry, W., 1961. No Title, in: Biochemists Handbook. E & FN Epon Led. Press, London, p. 83.

Duraipandy, N., Lakra, R., Kunnavakkam Vinjimur, S., Samanta, D., K, P.S., Kiran, M.S., 2014. Caging of plumbagin on silver nanoparticles imparts selectivity and sensitivity to plumbagin for targeted cancer cell apoptosis. Metallomics 6, 2025–2033. https://doi.org/10.1039/C4MT00165F.

Elokely, K.M., Doerksen, R.J., 2013. Docking challenge: protein sampling and molecular docking performance. J. Chem. Inf. Model. 53, 1934–1945. https://doi.org/10.1021/ci400040d.

Forster, T., Sinanoglu, O., 1965. No Title, in: Modern Quantum Chemistry. Academic Press, New York, pp. 93–137.

Gao, H., Lei, L., Liu, J., Kong, Q., Chen, X., Hu, Z., 2004. The study on the interaction between human serum albumin and a new reagent with antitumour activity by spectrophotometric methods. J. Photochem. Photobiol. A Chem. 167, 213–221. https://doi.org/10.1016/j.jphotochem.2004.05.017.

Hall, M.L., Jorgensen, W.L., Whitehead, L., 2013. Automated ligand- and structure-based protocol for in silico prediction of human serum albumin binding. J. Chem. Inf. Model. 53, 907–922. https://doi.org/10.1021/ci3006098.

Ibrahim, N., Ibrahim, H., Kim, S., Nallet, J.-P., Nepveu, F., 2010. Interactions between antimalarial indolone-N-oxide derivatives and human serum albumin. Biomacromolecules 11, 3341–3351. https://doi.org/10.1021/bm100814n.

Il'ichev, Y.V., Perry, J.L., Simon, J.D., 2002. Interaction of ochratoxin A with human serum albumin. preferential binding of the dianion and pH effects. J. Phys. Chem. B 106, 452–459. https://doi.org/10.1021/jp012314u.

Iqbal, S., Qais, F.A., Alam, M.M., Naseem, I., 2018. Effect of glycation on human serum albumin–zinc interaction: a biophysical study. J. Biol. Inorg. Chem. 23, 447–458. https://doi.org/10.1007/s00775-018-1554-8.

Ishtikhar, M., Khan, S., Badr, G., Osama Mohamed, A., Hasan Khan, R., 2014a. Interaction of the 5-fluorouracil analog 5-fluoro-2′-deoxyuridine with 'N' and 'B' isoforms of human serum albumin: a spectroscopic and calorimetric study. Mol. BioSyst. 10, 2954–2964. https://doi.org/10.1039/C4MB00306C.

Ishtikhar, M., Rabbani, G., Khan, R.H., 2014b. Interaction of 5-fluoro-5'-deoxyuridine with human serum albumin under physiological and non-physiological condition: a biophysical investigation. Colloids Surf. B Biointerfaces 123, 469–477. https://doi.org/10.1016/j.colsurfb.2014.09.044.

Kabir, M.Z., Feroz, S.R., Mukarram, A.K., Alias, Z., Mohamad, S.B., Tayyab, S., 2016. Interaction of a tyrosine kinase inhibitor, vandetanib with human serum albumin as studied by fluorescence quenching and molecular docking. J. Biomol. Struct. Dyn. 34, 1693–1704. https://doi.org/10.1080/07391102.2015.1089187.

Khan, M.S., Qais, F.A., Rehman, M.T., Ismail, M.H., Alokail, M.S., Altwaijry, N., Alafaleq, N.O., AlAjmi, M.F., Salem, N., Alqhatani, R., 2020. Mechanistic inhibition of non-enzymatic glycation and aldose reductase activity by naringenin: binding, enzyme kinetics and molecular docking analysis. Int. J. Biol. Macromol. 159, 87–97. https://doi.org/10.1016/j.ijbiomac.2020.04.226.

Khan, S.N., Islam, B., Yennamalli, R., Sultan, A., Subbarao, N., Khan, A.U., 2008. Interaction of mitoxantrone with human serum albumin: spectroscopic and molecular modeling studies. Eur. J. Pharm. Sci. 35, 371–382. https://doi.org/10.1016/j.ejps.2008.07.010.

Khatun, S., Riyazuddeen, Qais, F.A., 2019. In-vitro binding analysis of bovine serum albumin with sulindac/chlorpromazine: spectroscopic, calorimetric and computational approaches. J. Mol. Liq., 112124 https://doi.org/10.1016/j.molliq.2019.112124.

Kragh-Hansen, U., 1981. Molecular aspects of ligand binding to serum albumin. Pharmacol. Rev. 33, 17–53.

Li, Y., Yao, X., Jin, J., Chen, X., Hu, Z., 2007. Interaction of rhein with human serum albumin investigation by optical spectroscopic technique and modeling studies. Biochim. Biophys. Acta - Proteins Proteomics 1774, 51–58. https://doi.org/10.1016/j.bbapap.2006.09.020.

Liu, Y., Cai, Y., He, C., Chen, M., Li, H., 2017. Anticancer properties and pharmaceutical applications of plumbagin: a review. Am. J. Chin. Med. 45, 423–441. https://doi.org/10.1142/S0192415X17500264.

Lou, Y.-Y., Zhou, K.-L., Shi, J.-H., Pan, D.-Q., 2017. Characterizing the binding interaction of fungicide boscalid with bovine serum albumin (BSA): a spectroscopic study in combination with molecular docking approach. J. Photochem. Photobiol. B Biol. 173, 589–597. https://doi.org/10.1016/j.jphotobiol.2017.06.037.

Miller, J., 1979. Recent advances in molecular luminescence analysis. Proc. Anal. Div. Chem. Soc. 16, 203–208.

Mohammadi, T., Ghayeb, Y., Sharifi, T., Khayamian, T., 2017. The effect of dichlorvos on the structural alteration of serum albumins: a combined spectroscopic and molecular dynamic simulation approach. Monatshefte für Chemie - Chem. Mon. 148, 1141–1151. https://doi.org/10.1007/s00706-016-1857-9.

Morris, G.M., Goodsell, D.S., Halliday, R.S., Huey, R., Hart, W.E., Belew, R.K., Olson, A. J., 1998. Automated docking using a Lamarckian genetic algorithm and an empirical binding free energy function. J. Comput. Chem. 19, 1639–1662. https://doi.org/10.1002/(SICI)1096-987X(19981115)19:14<1639::AID-JCC10>3.0.CO;2-B.

Nusrat, S., Masroor, A., Zaman, M., Siddiqi, M.K., Ajmal, M.R., Zaidi, N., Abdelhameed, A.S., Khan, R.H., 2018. Interaction of catecholamine precursor l-Dopa with lysozyme: a biophysical insight. Int. J. Biol. Macromol. 109, 1132–1139. https://doi.org/10.1016/j.ijbiomac.2017.11.107.

Qais, F.A., Alam, M.M., Naseem, I., Ahmad, I., 2016. Understanding the mechanism of non-enzymatic glycation inhibition by cinnamic acid: an in vitro interaction and molecular modelling study. RSC Adv. 6, 65322–65337. https://doi.org/10.1039/C6RA12321J.

Rohs, R., 2005. Molecular flexibility in ab initio drug docking to DNA: binding-site and binding-mode transitions in all-atom Monte Carlo simulations. Nucleic Acids Res. 33, 7048–7057. https://doi.org/10.1093/nar/gki1008.

Shahabadi, N., Maghsudi, M., 2009. Binding studies of a new copper (II) complex containing mixed aliphatic and aromatic dinitrogen ligands with bovine serum albumin using different instrumental methods. J. Mol. Struct. 929, 193–199. https://doi.org/10.1016/j.molstruc.2009.04.027.

Siddiqui, S., Ameen, F., Jahan, I., Nayeem, S.M., Tabish, M., 2019. A comprehensive spectroscopic and computational investigation on the binding of the anti-asthmatic drug triamcinolone with serum albumin. New J. Chem. 43, 4137–4151. https://doi.org/10.1039/C8NJ05486J.

Sudlow, G., Birkett, D.J., Wade, D.N., 1975. The characterization of two specific drug binding sites on human serum albumin. Mol. Pharmacol. 11, 824–832.

Sułkowska, A., 2002. Interaction of drugs with bovine and human serum albumin. J. Mol. Struct. 614, 227–232. https://doi.org/10.1016/S0022-2860(02)00256-9.

Suryawanshi, V.D., Walekar, L.S., Gore, A.H., Anbhule, P.V., Kolekar, G.B., 2016. Spectroscopic analysis on the binding interaction of biologically active pyrimidine derivative with bovine serum albumin. J. Pharm. Anal. 6, 56–63. https://doi.org/10.1016/j.jpha.2015.07.001.

Trott, O., Olson, A.J., 2009. AutoDock Vina: improving the speed and accuracy of docking with a new scoring function, efficient optimization, and multithreading. J. Comput. Chem. 31, 455–461. https://doi.org/10.1002/jcc.21334.

Wang, Y.-Q., Zhang, H.-M., Zhang, G.-C., Tao, W.-H., Tang, S.-H., 2007. Interaction of the flavonoid hesperidin with bovine serum albumin: a fluorescence quenching study. J. Lumin. 126, 211–218. https://doi.org/10.1016/j.jlumin.2006.06.013.

Xu, L., Zhu, Y., Ma, W., Kuang, H., Liu, L., Wang, L., Xu, C., 2011. Sensitive and specific DNA detection based on nicking endonuclease-assisted fluorescence resonance energy transfer amplification. J. Phys. Chem. C 115, 16315–16321. https://doi.org/10.1021/jp2036263.

Yasmeen, S., Riyazuddeen, Qais, F.A., 2017. Unraveling the thermodynamics, binding mechanism and conformational changes of HSA with chromolyn sodium: Multispecroscopy, isothermal titration calorimetry and molecular docking studies. Int. J. Biol. Macromol. 105, 92–102. https://doi.org/10.1016/j.ijbiomac.2017.06.122.

Zaman, M., Safdari, H.A., Khan, A.N., Zakariya, S.M., Nusrat, S., Chandel, T.I., Khan, R. H., 2019. Interaction of anticancer drug pinostrobin with lysozyme: a biophysical and molecular docking approach. J. Biomol. Struct. Dyn. 37, 4338–4344. https://doi.org/10.1080/07391102.2018.1547661.

Zhang, Y.-Z., Zhou, B., Liu, Y.-X., Zhou, C.-X., Ding, X.-L., Liu, Y., 2008. Fluorescence study on the interaction of bovine serum albumin with P-aminoazobenzene. J. Fluoresc. 18, 109–118. https://doi.org/10.1007/s10895-007-0247-4.

Zia, M.K., Siddiqui, T., Ali, S.S., Rehman, A.A., Ahsan, H., Khan, F.H., 2018. Chemotherapeutic drugs and plasma proteins: exploring new dimensions. Curr. Protein Pept. Sci. 19, 937–947. https://doi.org/10.2174/1389203718666171002115547.